This article has been accepted for publication in a future issue of this journal, but has not been fully edited. Content may change prior to final publication. Citation information: DOI 10.1109/TPWRD.2018.2888597, IEEE Transactions on Power Delivery

Improved Method for Acoustic Identification of Free Conductive Particle Defects in GIL

Zhicheng Wu*, *Student Member, IEEE*, Qiaogen Zhang, Jiajie Song, Xiaoang Li

***Abstract*-- The presence of free conductive particles in gas-insulated transmission lines (GIL) is the most significant threat to their insulation. The non-invasive identification of free conductive particle defects in GILs is extremely challenging. Existing identification methods which use the acoustic amplitude-flight time (AAFT) pattern are not often adopted on-site due to their faulty theory, non-robust extraction algorithm, and generally inaccurate calibration. In this study, the theory established by L. E. Lundgarrd is expanded by deriving estimation equations related to the particle's moving state. A new method for extracting the state information from the raw data of acoustic signals is established and the robustness of the acoustic identification method is enhanced. A convenient calibration method is also developed by building a standard collision signal generator. The proposed methods are validated in a scale GIL model and a real GIL model. The results of this study may represent a workable reference for GIL condition monitoring.**

***Index Terms*-- Partial discharges, Acoustic signal processing, Equipment failure, Gas insulation**

I. Nomenclature

Symbol	Description	Unit
A	Acoustic signal amplitude	V
a_q	Acceleration due to Coulomb force	$m \cdot s^{-2}$
C_R	Coefficient of restitution	
$\hat{E}$	Modulus of electric field	$V \cdot m^{-1}$
g	Constant of gravitation	$m \cdot s^{-2}$
H	Height of electromagnet chuck and enclosure	m
h_{max}	Maximum particle flight height	m
$\tilde{h}_{max}$	Maximum particle flight height (estimated value)	m
k_s	Sensor sensitivity of whole measurement system	$V \cdot kg^{-1} \cdot m^{-1} \cdot s$
l	Linear particle length	m
m	Particle mass	kg
$\tilde{m}$	Particle mass (estimated value)	kg
q_{max}	Maximum particle charge	C
$\tilde{q}_{max}$	Maximum particle charge (estimated value)	C
r	Spherical particle radius	m
t	Duration of one particle flight	s
v_n	Collision velocity of particles with enclosure	$m \cdot s^{-1}$
Δv_{max}	Maximum particle velocity increment	$m \cdot s^{-1}$
Φ	Linear particle diameter	m
ω	Angular frequency of oscillating electric field	$rad \cdot s^{-1}$

II. Introduction

THE presence of free conductive particles in the gas-insulated transmission line (GIL) is the most significant threat to its insulation [1]-[5]. According to a survey by CIGRE 33/23.12, insulation failures due to particles and foreign bodies represent 20% of the total in SF_6 gas insulated systems [6]. Under the influence of applied electric field or mechanical vibration, the particles may move along the enclosure and/or attach to the spacer surface to cause a flashover under the operating voltage. For example, a sudden flashover among the insulator surfaces in the 363 kV Antong substation (Qinghai Province, P. R. China) during normal operation was the result of a discharge fault of the free conductive particles deposited on the insulator surface [7]. Particles attracted to the HV electrode or deposited on the surface of the insulator can result in a very low breakdown level while creating a highly divergent field. The threat of free conductive particles should be carefully considered throughout the life cycle of the GIL.

It is very challenging to identify free conductive particle defects in GILs in a non-invasive manner [8]-[9]. The unit length of the GIL is greater than 10 m and the enclosure is generally welded closed [10]. Opening a larger GIL unit to determine the existence of free conductive particles is very costly compared to the use of gas-insulated metal-enclosed switchgear (GIS). The identification of free conductive particle defects in GILs, ideally done on-line, is a problem which urgently demands a solution in terms of safe, effective GIL equipment.

Acoustic methods are usually performed on-site or for online monitoring and diagnosis in the form of partial discharge tests for GILs throughout the life cycle of the equipment [10]. It is widely accepted that the acoustic method is more sensitive to free particles than other available partial discharge measurement methods, due to the direct collision between particles and GIL enclosure. However, traditional acoustic methods can only be used as qualitative detection methods, but not for accurate quantitative identification. Finding the quantitative correlations between acoustic signal and equipment failure risk is a major challenge.

The acoustic amplitude-flight time (AAFT) pattern can be used to assess the condition of GILs per the existence of free conductive particles. In 1995, H. D. Holmberg found that flight time (i.e., the temporal interval between two adjacent collisions)

This work was supported in part by the Science and Technology Project of China Southern Power Grid Co. Ltd. (Contract number: ZBKJXM20170059).

Z. Wu, Q. Zhang, J. Song, and X. Li are with the State Key Laboratory of Electric Insulation and Power Equipment, Xi'an Jiaotong University, Xi'an 710049, P. R. China (e-mail: z_c_wu@163.com).

This article has been accepted for publication in a future issue of this journal, but has not been fully edited. Content may change prior to final publication. Citation information: DOI 10.1109/TPWRD.2018.2888597, IEEE Transactions on Power Delivery

can be used to estimate the risk of free conductive particle defects [11]. Later, M. Runde qualitatively analyzed the moving mode of particles by using the AAFT pattern [12]. In 2001, L. E. Lundgarrd investigated the relationship between the AAFT pattern and particle properties to establish several estimation equations including particle mass and particle charge [13]. It should be noted that there are several problems with these scholars' results, leading to a lack of use of the acoustic methods in further fault diagnosis. First, these results are based on scale models without necessary validation on a real GIL model. Further, sensor sensitivity calibration cannot be conveniently performed on-site. These methods are also lacking in robustness, i.e., they can only detect defects above a specific severity threshold and require a very lengthy test to effectively plot the AAFT pattern. In short: these methods are not commonly adopted before certain optimizations. Hence, the free conductive particle defect are still a tricky problem for gas-insulated equipment, especially GIL equipment with a long distance.

This paper proposes an improved method for acoustic identification of free conductive particle defects in GIL. Three main challenges were addressed in conducting the present study. First, an estimated equation directly linked to the failure risk of the equipment must derived in addition to the precise acquisition of particle properties. Second, existing methods are limited by the specific shape of the AAFT pattern and thus fail when applied voltage is low; a method with better robustness in particle property extraction from acoustic signal raw data was designed to account for this. Third, a normalized measurement method of acoustic measurement system sensitivity was established during an on-site test to enhance the measurement accuracy.

The contributions of this paper can be summarized as follows. 1) The theory established by L. E. Lundgarrd is expanded by deriving estimation equations related to the particle's moving state (Section 3). 2) A new method is established for robustly extracting state information from the raw data of acoustic signals (Section 4). 3) A convenient calibration method is developed by building a standard collision signal generator (Section 5). These techniques were validated in a scale GIL model and a real GIL model (Section 6). The proposed method allows for feasible and effective GIL condition monitoring.

III. Expanded Theory

This section discusses the correction and expansion of estimated equations derived by L. E. Lundgarrd, including the estimated equation of maximum of flight height which is directly linked to the failure risk of equipment. The equations were validated by experimental and numerical calculation results.

Based on the theory established by Lundgarrd, the amplitude of the acoustic signal measured by the acoustic emission (AE) sensor is proportional to the momentum of particle collision [13]:

$$A = k_s m v \tag{1}$$

The AAFT pattern can be decomposed into a linear component (passing through the zero point) and a sinusoidal component with power frequency (50 Hz or 60 Hz) according to results obtained by experiment and by numerical calculations. The maximum and minimum values appear to alternate with the flight time. The maximum envelope line value appears at three quarters of the period; the flight time is $0.02n+0.15$ ($n \geqslant 0$). The minimum values appear at a quarter of the period; the flight time is $0.02n + 0.05$ ($n \geqslant 0$). The minimum upper envelope value and maximum lower envelope value on each period forms a straight line passing through the zero point, i.e., the linear component mentioned above. In mathematic language, the upper and lower envelopes are:

$$A = \mathrm{C}_1 t + \mathrm{C}_2 \left[\sin(\omega t - \pi) + 1\right] \tag{2}$$

$$A = \mathrm{C}_1 t + \mathrm{C}_2 \left[\sin(\omega t - \pi) - 1\right] \tag{3}$$

Free particle movement under AC voltage can be calculated according to previously published methods [14]. The particle charge after each collision with different colors is shown in Figure 1. The linear component was formed by the electrically neutral particles, and the sinusoidal component was formed by the particle with largest charge.

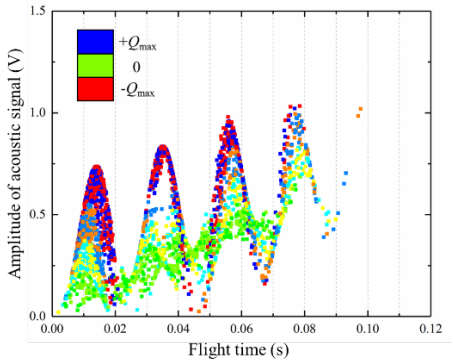

Figure 1. Typical AAFT pattern marked with particle charge. Green points indicate electrically neutral particles; red or blue points indicate maximum or minimum charge on the particle, respectively.

The constant C_1, as-derived from the movement of the electrically neutral particles, is proportional to the particle mass:

$$\mathrm{C}_1 = \frac{1}{2} g k_s m \tag{4}$$

The effect of oscillating electric field force on particle movement should be reflected in the expression of constant C_2. In Lundgarrd's opinion, the velocity component caused by the Coulomb forces reaches its maximum when the particle hits the enclosure after having completed a full half cycle of the same polarity it had when taking off. This is not actually the case; further, this caused non-negligible error between his experiment and estimation equations (Figure 16, [13]).

This article has been accepted for publication in a future issue of this journal, but has not been fully edited. Content may change prior to final publication. Citation information: DOI 10.1109/TPWRD.2018.2888597, IEEE Transactions on Power Delivery

The amplitude of the sinusoidal component in the AAFT pattern corresponds to the maximum particle velocity under Coulomb forces, but the particles must receive maximum discharge from the collision to obtain the maximum speed, i.e., the collision time should be located at the positive peak of the voltage. The relationship between such acceleration, velocity, and instantaneous voltage is shown in Figure 2. The maximum velocity appears at a quarter cycle, not a half cycle. The particle velocity deceases when the flight time exceeds a quarter cycle, so the maximum velocity increment $\Delta v_{\max}$ of the particle can be obtained by integrating the acceleration over a quarter period:

$$\Delta v_{\max} = \int_0^{\frac{T}{4}} a_{\mathrm{q}} dt = \frac{q_{\max}\hat{E}}{\omega m} \tag{5}$$

The constant C_2 is expressed by combining (1) and (5) to form (6):

$$\mathrm{C}_2 = \frac{1}{2} k_s \Delta v = \frac{k_s q_{\max}\hat{E}}{2\omega} \tag{6}$$

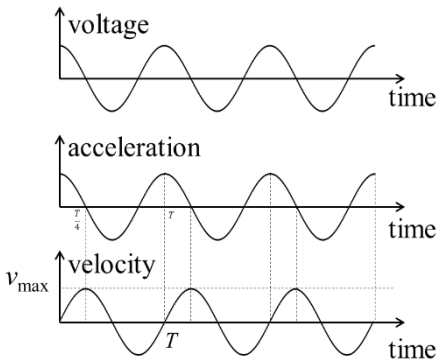

Figure 2. Relationship between acceleration, velocity, and instantaneous voltage (gravity-free condition); maximum particle velocity appears at quarter period.

To validate the above analysis, theoretical expressions of AAFT pattern envelope lines were compared to numerical and experimental results (Figure 3, black dashed lines). The theoretical AAFT pattern expressions are consistent with the numerical and experimental results. This proves that the correction to L. E. Lundgarrd's theory is correct.

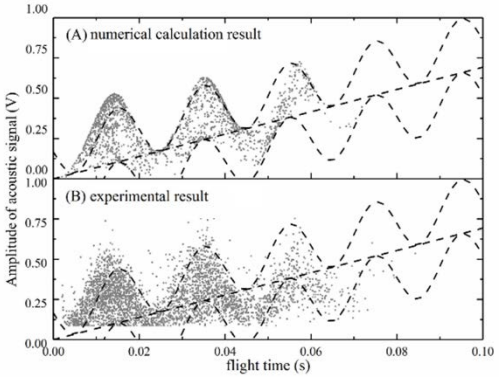

Figure 3. Experimental and numerical calculations for comparison against AAFT. Results based on a spherical particle with 1 mm diameter in 18 mm/88 mm coaxial cylinder electrode system under 75 kV.

Once the AAFT pattern is plotted, the particle properties (including mass and charge) can be identified by fitting the envelope lines of the pattern and solving (2) and (3). However, if the envelope lines cannot be recognized, identification by fitting the envelope fails due to over-dependency on the specific AAFT pattern shape. The solution of this case will be illustrated in next section.

The express purpose of condition monitoring is assessing the condition of GIL equipment. The mass or charge of particles do not directly reflect the risk of equipment failure. It is necessary to derive further estimation equations of the physical quantities directly linked to the failure risk.

In an actual GIL free conductive particle defect scenario, the particle movement may include multiple collisions. The rebound velocity decays to the product of collision velocity and coefficient of restitution upon each collision. According to the above analysis, there exists a maximum velocity increment between the two collisions as shown in (5). The maximum rebound velocity of the (n+1)-th collision can be expressed by the velocity of the n-th collision:

$$v_{\mathrm{n+1}} = C_{\mathrm{R}} v_{\mathrm{n}} + \Delta v_{\max} \tag{7}$$

It is assumed that the maximum velocity increment can be obtained for each collision of the particle. As collision count n tends toward infinity, the maximum velocity $v_{\max}$ of the particle under the electric field can be calculated as follows:

$$v_{\max} = \lim_{n\to\infty} v_n = \frac{\Delta v_{\max}}{1-\mathrm{C}_{\mathrm{R}}} \tag{8}$$

Due to the limit on the velocity increment by Coulomb force, the influence of the electric field can be ignored. The maximum flight height $h_{\max}$ can be approximated as follows:

$$h_{\max} \approx \frac{v_{\max}^2}{2\mathrm{g}} \tag{9}$$

Particles moving close the busbar inevitably cause substantial electric field distortion and place the equipment in a very dangerous situation. The maximum of flight height $h_{\max}$ may thus be a better indication of failure probability in the GIL equipment.

Equations of the AAFT pattern envelope lines are now derived and particle properties can be estimated by solving (4) and (6). The estimation equations (e.g., maximum flight height) directly correspond to the failure risk of equipment.

IV. Robust Extraction

Particle properties can be identified by fitting the envelope lines of the complete AAFT pattern and solving the equations presented in Section 3. However, this approach is not applicable on-site. There are three reasons: The first is that the former

This article has been accepted for publication in a future issue of this journal, but has not been fully edited. Content may change prior to final publication. Citation information: DOI 10.1109/TPWRD.2018.2888597, IEEE Transactions on Power Delivery

methods are limited by the specific shape of the AAFT pattern and fail in the case of low applied voltage. For example, when the applied voltage is only slightly higher than the take-off voltage of a particle, the envelope lines cannot be fitted from the AAFT pattern (Figure 8(a)). Thus there is demand for a more general method of extracting particle properties from the raw data of acoustic signals. The second is that the former method also takes a long time – sometimes too long – to plot an AAFT pattern of sufficient quality. At last, the on-site mechanical noises would blur the AAFT pattern and make it difficult to fit the key parameters for next analysis. Therefore, a more robust signal processing method is urgently needed to process the raw data.

As per the analysis in Section 3, the AAFT pattern shape is used to solve the particle parameters, while the relationship between two adjacent collision signals is neglected. But the acoustic signal of two adjacent collision events show a strong correlation due to the continuity of particle movement. This characteristic was exploited in this study to establish a method with enhanced robustness for extracting particle properties. The proposed method is unrestricted by measurement time and pattern shape in obtaining accurate particle properties.

The theoretical basis of this method should be clarified at first. That is, there exists a limit to the effect of the electric field force on the velocity of a particle as it moves. The basic assumption is that the effect of the electric field force on the particle's movement during a single flight is not significant. The effect of the collision phase on the flight time of the next movement was calculated here as shown in Figure 4. The flight time with the collision phase changes in an offset sine-wave manner; the sinusoidal amplitude is much smaller than the offset amplitude. The physical meaning of this offset is the flight time under gravity-only conditions. The uniform distribution of the collision phase makes the effect of the electric field force negligible in the case of large samples. That is, the single movement of the particle can be approximated as an upthrow with a specific initial velocity. The duration of the movement depends on the initial velocity of the particle leaving the enclosure.

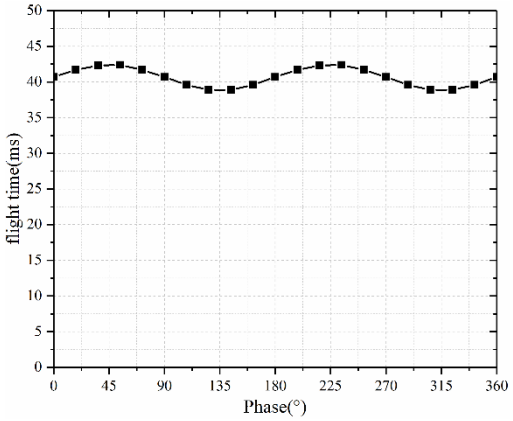

Figure 4. Relationship between collision phase and flight time by numerical calculation. Note: sinusoidal component is far smaller than the offset.

Based on the above hypothesis, the collision velocity of particles with the enclosure can be approximated as follows depending on the flight time:

$$v = g\frac{\Delta t}{2} \tag{10}$$

The following expression of the estimated particle mass $\tilde{m}$ is obtained by combining (1) and (10):

$$\tilde{m} = \frac{\mathrm{A}}{k_{\mathrm{s}} v} = \frac{2A}{k_{\mathrm{s}} \mathrm{g} \Delta t} \tag{11}$$

The effect of the electric field force can be ignored when dealing with large samples due to the uniform distribution of the collision phase. Thus, the percentile filter can be used to smooth the results of (13) as the final estimation. The filter here is another important source of robustness, which filters out sporadic interfering signals. The recommended percentile filter parameters are 100 window points and 30 percentiles.

The limit of the velocity increment under the influence of electric field force is Δv during a single flight, as shown in (5). Corresponding to the sequence of acoustic collision signals, the velocity increment Δv of the particle in the single movement can be expressed by two adjacent collision acoustic amplitudes as shown in (12). Aluminum is a common GIL material; its coefficient of restitution is 0.5.

$$\Delta v = \frac{A_{\mathrm{n+1}} - C_{\mathrm{R}} A_{\mathrm{n}}}{k_{\mathrm{s}}} \tag{12}$$

The estimated charge $\tilde{q}_{\max}$ is defined by (13) according to (1), (5), and (12):

$$\tilde{q}_{\max} = \max[\frac{\omega(A_{i+1} - C_{\mathrm{R}} A_i)}{k_{\mathrm{s}} E_{\mathrm{p}}}] \tag{13}$$

To prevent outliers from affecting the results, the percentile filter can be used to replace the maximum function in (15). The recommended percentile is 0.9.

The maximum flight height can be estimated ignoring the effect of electric field force on the particle. The maximum flight height $\tilde{h}_{\max}$ is:

$$\tilde{h}_{\max} = \max(\frac{g\Delta t^2}{8}) \tag{14}$$

These three estimation equations were derived to obtain the particle properties of mass, charge, and maximum flight height. The relationship between adjacent acoustic signals was exploited to overcome the limitations of previously published methods. With the help of percentile filter, the robustness of this

This article has been accepted for publication in a future issue of this journal, but has not been fully edited. Content may change prior to final publication. Citation information: DOI 10.1109/TPWRD.2018.2888597, IEEE Transactions on Power Delivery

new method has been further improved. The proposed method allows particle information to be extracted from acoustic signal raw data at enhanced robustness.

V. ACCURATE CALIBRATION

According to the above analysis, the particle mass and particle charge are closely related to the sensitivity of the acoustic measurement system. This sensitivity must be calibrated to accurately obtain the particle characteristics.

The measured acoustic signal is not only related to the sensitivity of the AE sensor but also to measurement conditions such as the enclosure material. It is necessary to calibrate the sensitivity of the whole acoustic measurement system in situ.

Several authors have reported calibration methods which exploit the relationship between the time interval and acoustic signal amplitude when a known particle is free-falling and hits the enclosure [4][13][16]. The sensitivity can be expressed as follows:

$$k_s = \frac{2A}{gm\Delta t} \tag{15}$$

However, this approach is inherently flawed. The particle inevitably collides with the shell obliquely due to the curvature of the enclosure. The tangential velocity caused by the oblique impact increases the collision time interval, resulting in a large sensitivity error. In addition, this method is not easily implemented on-site. To facilitate an accurate measurement of acoustic measurement system sensitivity, a standard collision signal generator is recommended for on-site tests.

The standard collision signal generator consists of an electromagnet chuck, control circuits, and a steel particle of known mass. A schematic diagram of the generator is shown in Figure 5. The control circuit generates a repeatable square wave with a period of about 1.5 s and a duty cycle of about 10%. A relay is controlled by this square wave which determines whether the electromagnet chuck is working or not. When the electromagnet chuck works, the steel particles are attracted to the chuck. When the electromagnet chuck loses power, the particles fall freely from a known height and collide with the GIL enclosure to produce a standard collision signal.

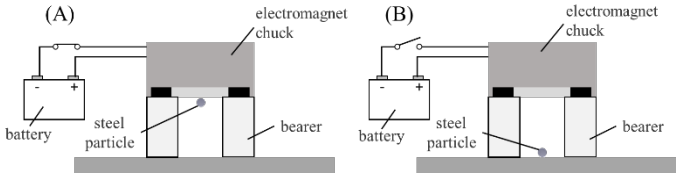

Figure 5. Standard collision signal generator applied to calibrate acoustic measurement system.

The measurement is fully automated to generate a series of accurate and stable collision signals. The standard collision signal waveforms generated by the generator mentioned above are shown in Figure 6.

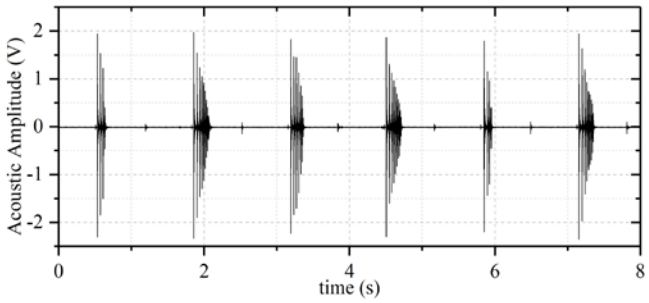

Figure 6. Standard collision signal waveforms created by generator.

The sensitivity of the acoustic measurement system k_s is:

$$k_s = \frac{A}{m\sqrt{2g(H-2r)}} \tag{16}$$

Once the calibrated acoustic sensitivity has been obtained, the particle properties can be extracted by the methods described above.

VI. METHOD VALIDATION

To validate the correctness and feasibility of the proposed method, a series of experiments was carried out in a scale GIL model and a real GIL model. The experimental platform was set up as shown in Figure 7.

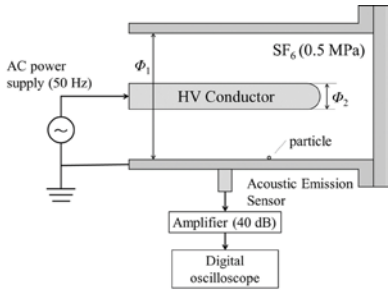

Figure 7. Experimental platform diagram.

Coaxial cylinder systems were used as an experimental chamber. The scale model has an inner conductor diameter of 18 mm and an enclosure diameter of 88 mm. The real model has an inner conductor diameter of 140 mm and an enclosure diameter of 560 mm. Both GIL models were filled with 0.5 MPa SF_6. The inner conductor was connected to a 400 kV/90 kVA gas-insulated transformer. The frequency of applied voltage was 50 Hz.

The acoustic signal acquisition system is mainly composed of an AE sensor, preamplifier, and oscilloscope. The AE sensor (model: Soundwel SR40M) was selected with a resonant frequency of 40 kHz to keep the measurement frequency between 20 kHz and 100 kHz. The preamplifier has a bandwidth of 10 kHz to 2 MHz, gain of 40 dB, and input impedance over 50 MΩ. A Tektronix® DPO4104 oscilloscope with a bandwidth of 1 GHz and a sampling rate of 5 GS/s was used to acquire acoustic signals; the acoustic signal was

This article has been accepted for publication in a future issue of this journal, but has not been fully edited. Content may change prior to final publication. Citation information: DOI 10.1109/TPWRD.2018.2888597, IEEE Transactions on Power Delivery

continuously measured for 100 seconds at a sampling rate of 100 kS/s.

The standard collision signal generator described above was fixed on the enclosure of the GIL model to calibrate the acoustic measurement system. The arrangement of the AE sensor and standard collision signal generator is shown in Figure 8. After calibration, the sensitivities of the measurement system were measured in both the scale and real model as 1.03×10^5 V·kg^{-1}·m^{-1}·s and 2.83×10^5 V·kg^{-1}·m^{-1}·s, respectively.

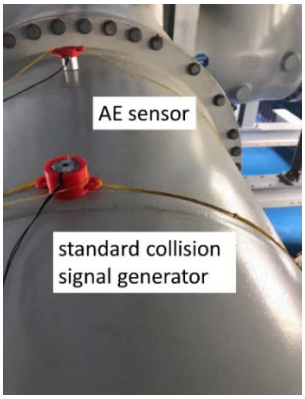

Figure 8. Arrangement of AE sensor and standard collision signal generator.

All experiments were performed as a double-blind trial wherein the analyst did not know what data was to be analyzed for which types of particles. In the scale model, aluminum spheres with diameters of 0.5 mm, 1.0 mm, and 1.5 mm were used to simulate free conductive particle defects. Several experiments were carried out under different voltages for each type of particle. The AAFT patterns extracted from the acoustic signals are shown in Figure 9. The estimated results using (11) and (13) are given in Table 1 and Table 2 for comparison with the actual values. The improved method provided very high accuracy particle mass (+1.45%) and particle charge (-1.54%) information for a 1 mm diameter spherical particle under 45 kV applied voltage. This information cannot be extracted by fitting the envelope lines in Figure 9(a), which reflects the enhanced robustness of the proposed method.

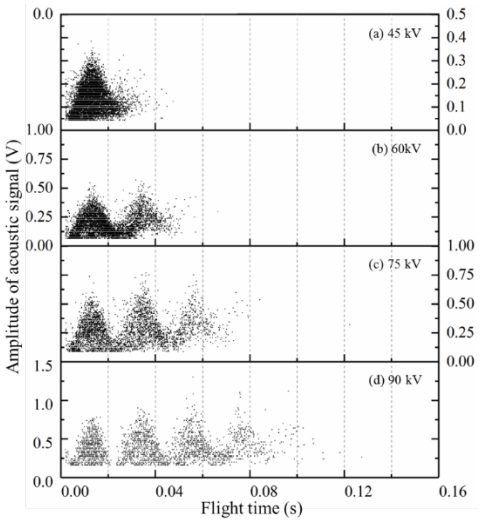

Figure 9. AAFT patterns obtained in scale GIL model. Results based on a spherical particle with 1 mm diameter in 18 mm/88 mm coaxial cylinder electrode system under 45 kV to 90 kV power frequency voltage. Note: the vertical axes of each subfigure differ.

Table 1. Estimated versus actual mass (Scale model)

Particle Diameter (mm)	Voltage (kV)	Estimated mass (μg)	Actual mass (μg)	Fractional error (%)
0.5	26	1.41	1.41	-0.11
	32	1.46		+3.04
	42	1.35		-4.67
	53	1.35		-4.40
	63	1.34		-5.06
	74	1.37		-3.20
1.0	37	11.84	11.31	+4.73
	45	11.47		+1.45
	60	10.73		-5.09
	75	10.75		-4.97
	90	10.44		-7.66
1.5	45	47.02	38.17	+23.19
	55	46.49		+21.79
	73	38.57		+1.05
	91	36.68		-3.91
	110	37.24		-2.42
	127	36.65		-3.99

Table 2. Estimated versus actual charge (Scale model)

Particle Diameter (mm)	Voltage (kV)	Estimated charge (pC)	Actual charge (pC)	Fractional error (%)
0.5	26	6.49	6.02	7.73
	32	6.51	7.41	-12.17
	42	7.13	9.73	-26.74
	53	8.62	12.27	-29.79
	63	9.00	14.59	-38.29
	74	9.90	17.14	-42.23
1.0	37	38.50	34.27	+12.32
	45	41.05	41.68	-1.54
	60	44.37	55.58	-20.16
	75	50.21	69.47	-27.73
	90	57.46	83.36	-31.07
1.5	45	95.81	93.78	2.16
	55	103.94	114.63	-9.32
	73	106.45	152.14	-30.03
	91	116.52	189.65	-38.56
	110	131.26	229.25	-42.75
	127	143.67	264.68	-45.72

Two kinds of particles were used in the real-model experiments: spherical (Φ = 1.0 mm) and linear (Φ = 0.4 mm, l = 5 mm). In practice, linear particles are more common than spherical particles. The applied voltage was 330 kV rms for spherical particles. The estimated mass is 1.13 μg (actual value: 1.41 μg) and the estimated charge is 66.2 pC (actual value: 55.0 pC), respectively. Three applied voltages were tested for linear particles. The estimated and actual values are shown in Table 3.

Table 3. Estimated versus actual mass (Real model)

Voltage (kV)	Estimated mass (μg)	Actual mass (μg)	Fractional error (%)
150	1.34	1.41	-4.96
100	1.21		-14.18
250	1.65		+17.02

The particle mass error is within about 5% in the scale model and within 20% in the real model, which suggests that (11)

yields accurate particle mass estimations. According to Table 2, the particle charge estimations become inaccurate under higher voltages; there is a significant decline in fractional error as voltage increases. The electric field strength at the surface of the enclosure serves as an estimate in (24), which produces relatively large error as the particles can move to a higher position at higher voltages. In a word, the proposed method has stronger accuracy for particle properties under lower applied voltages than the traditional method. Stepwise voltage application is recommended for the acoustic identification of free conductive particle defects via this approach during on-site dielectric test.

VII. Conclusion

This paper discussed expanded theory, robust extraction, and accuracy calibration for improving the acoustic identification of free conductive particles in GIL equipment. The results can be summarized as follows.

1) The estimated equations derived by L. E. Lundgarrd were corrected and expanded. The maximum velocity increment was expressed by integrating the acceleration over a quarter period instead of a half cycle. An equation for maximum flight height which effectively facilitates a failure probability prognosis for GIL equipment was derived.

2) The strong correlation between adjacent collision signals was exploited to instead extract the particle properties unrestricted by measurement time or pattern shape. With the help of percentile filter, the robustness of this new method has been further improved. Particle properties under lower applied voltage can be obtained accurately via the proposed method.

3) To facilitate an accurate measurement of acoustic measurement system sensitivity, a standard collision signal generator is recommended during on-site tests to generate a series of accurate and stable collision signals.

4) Validation experiments indicated that the error of particle mass is within 5% in the scale model and within 20% in the real model. In other words, all three parts of the proposed method, including expanded theory, robust extraction and accurate calibration, are applicable.

VIII. References

[1] A. H. Cookson, "Electrical breakdown for uniform fields in compressed gases", *Proc. IEE*, Vol. 117, No. 1, pp. 269-280, 1970.
[2] K. D. Srivastava and M. M. Morcos, "A review of some critical aspects of insulation design of GIS/GIL systems", *IEEE/PES Transmission and Distribution Conference and Exposition*. pp. 787-792, 2001.
[3] M. M. Morcos, S. A. Ward, H. Anis, K. D. Srivastava and S. M. Gubanski, "Insulation integrity of GIS/GITL systems and management of particle contamination", *IEEE Elect. Insul. Mag.*, Vol. 16, No. 5, pp. 25-37, 2000.
[4] J. Wang, Q. Li, B. Li, C. Chen, S. Liu and H. Ji, "Motion analysis of spherical metal particle in AC gas-insulated lines: random effects and resistance of the SF_6/N_2 mixture", *IEEE Trans. Dielectr. Electr. Insul.*, Vol. 23, No. 5, pp. 2617-2625, 2016.
[5] T. Sangsri and B. Techaumnat, "Experimental study on the movement of non-spherical particles in nonuniform electric field", *IEEE Trans. Dielectr. Electr. Insul.*, V ol. 24, no. 2, pp. 861-868, 2017.
[6] CIGRE JWG 33/23.12. "Insulation co-ordination of GIS: Return of Experience, On Site Tests and Diagnostic Techniques", *Electra*, No. 176, pp. 67-97, 1998.
[7] S. Xu, K. Meng and W. Liu, "Analysis of 363 kV Gas Insulated Switchgear Charging Flashover Fault", *High Voltage Apparatus*, Vol. 43, No. 1, pp. 74-76, 2007.
[8] M. Wübbenhorst and J. van Turnhout, "Special issue of the IEEE transactions on dielectrics and electrical insulation electrets and related phenomena", *IEEE Trans. Dielectr. Electr. Insul.*, Vol. 24, No. 3, pp. 1974-1974, 2017.
[9] *High-voltage Test Techniques – Partial Discharge Measurements*, IEC 60270, 2015.
[10] L. E. Lundgaard, G. Tangen, B. Skyberg and K. Faugstad, "Acoustic diagnoses of GIS; field experience and development of expert system", *IEEE Trans. Power Del.*, Vol. 7, No. 1, pp. 287-294, 1992.
[11] H. D. Schlemper and K. Feser, "Estimation of mass and length of moving particles in GIS by combined acoustical and electrical PD detection", *Proceedings of Conference on Electrical Insulation and Dielectric Phenomena (CEIDP)*, pp. 90-93, 1996.
[12] M. Runde, T. Aurud, K. Ljokelsoy, L. E. Lundgaard, "Risk assessment basis of moving particles in gas insulated substations", *IEEE Trans. Power Del.*, Vol. 12, No. 2, pp. 714-721, 1997.
[13] L. E. Lundgaard, G. Tangen, B. Skyberg and K. Faugstad, "Acoustic diagnoses of GIS; field experience and development of expert system", *IEEE Trans. Power Del.*, Vol. 7, No. 1, pp. 287-294, 1992.
[14] Z. Wu, Q. Zhang, J. Song, J. Ma, Q. Du, C. Gao, G. Wang and Y. Zhang, "Simulation and motion analysis of spherical free conducting particle between coaxial electrodes", *1st International Conference on Electrical Materials and Power Equipment (ICEMPE)*, pp. 324-327, 2017.
[15] H. Ji, C. Li, Z. Pang, B. Qi and S. Zheng, "Influence of Voltage Waveforms on Partial Discharge Characteristics of GIS Mobilized Metal Particles", *Trans. of China Electrotechnical Society*, Vol. 31, No. 13, pp. 218-226, 2016.

Zhicheng Wu (S'18) was born in Yunnan, China in 1993. He received a B.S. degree in computer science and technology from Xi'an Jiaotong University, Shaanxi, China in 2015. He is currently working toward a Ph.D. at the High Voltage Division, School of Electrical Engineering, and the State Key Laboratory of Electrical Insulation and Power Equipment. His research interest is technology for GIS/GIL defect detection.

Qiaogen Zhang received B.S., M.S., and Ph.D. degrees in electrical engineering from Xi'an Jiaotong University, Xi'an, China, in 1988, 1991, and 1996, respectively. He is currently a Professor with the High Voltage Division, School of Electrical Engineering, and the State Key Laboratory of Electrical Insulation and Power Equipment, Xi'an Jiaotong University. His major research interests include insulation structure design, power transmission and transformation technology, and insulation state evaluation.

Jiajie Song was born in Shanxi, China in 1995. She received a B.S. degree from Xi'an Jiaotong University, Shaanxi, China in 2017. Since 2017, she has been a graduate student in the State Key Laboratory of Power Equipment and Electrical Insulation, Xi'an Jiaotong University. Her main research interest is eco-efficient gas insulated switchgear.

Xiaoang Li was born in Shaanxi Province, China, in May 1989. He received the B.S. degree and Ph.D. degree in Electrical Engineering from Xi'an Jiaotong university, Xi'an, China, in 2011 and 2016 respectively. He is now a research assistant in the State Key Laboratory of Electrical Insulation and Power Equipment, Xi'an Jiaotong University, Xi'an, China. His mainly research interest is pulsed power technology and its applications.

This article has been accepted for publication in a future issue of this journal, but has not been fully edited. Content may change prior to final publication. Citation information: DOI 10.1109/TPWRD.2018.2888597, IEEE Transactions on Power Delivery